AJNR

Magnetic Resonance Imaging of Brain Iron

Burton Drayer, Peter Burger, Robert Darwin, Stephen Riederer, Robert Herfkens and G. Allan Johnson

AJNR Am J Neuroradiol 1986, 7 (3) 373-380
http://www.ajnr.org/content/7/3/373

Magnetic Resonance Imaging of Brain Iron

Burton Drayer[1,2]
Peter Burger[3]
Robert Darwin[1]
Stephen Riederer[1]
Robert Herfkens[1]
G. Allan Johnson[1]

A prominently decreased signal intensity in the globus pallidum, reticular substantia nigra, red nucleus, and dentate nucleus was routinely noted in 150 consecutive individuals on T2-weighted images (SE 2000/100) using a high field strength (1.5 T) MR system. This MR finding correlated closely with the decreased estimated T2 relaxation times and the sites of preferential accumulation of ferric iron using the Perls staining method on normal postmortem brains. The decreased signal intensity on T2-weighted images thus provides an accurate in vivo map of the normal distribution of brain iron. Perls stain and MR studies in normal brain also confirm an intermediate level of iron distribution in the striatum, and still lower levels in the cerebral gray and white matter. In the white matter, iron concentration is (a) absent in the most posterior portion of the internal capsule and optic radiations, (b) higher in the frontal than occipital regions, and (c) prominent in the subcortical "U" fibers, particularly in the temporal lobe. There is no iron in the brain at birth; it increases progressively with aging. Knowledge of the distribution of brain iron should assist in elucidating normal anatomic structures and in understanding neurodegenerative, demyelinating, and cerebrovascular disorders.

It has been suggested that magnetic resonance (MR), aside from producing exquisite anatomic images, may also provide unique biochemical information about brain function. Early attempts at Na-23 and P-31 imaging and spectroscopy have been promising but time-consuming. Initial studies of T1 and T2 relaxation times using proton MR imaging have proved highly feasible in a reasonable imaging time, but they have been disappointing in terms of specificity for lesion differentiation. When using a high field strength (1.5 T) MR unit, a consistent finding was apparent in every patient studied on a T2-weighted or calculated T2 image. This normal finding consisted of decreased signal intensity (decreased T2 relaxation time) in specific brain locales, including the globus pallidum, reticular substantia nigra, red nucleus, dentate nucleus, and putamen [1]. This paper gives an account of our studies to determine the origin of this biochemical effect.

Materials and Methods

MR images were reviewed from 150 consecutive brain studies in patients ranging in age from 8 years to 76 years. Various pathologies were present in all but 21 patients who had normal neurologic and MR examinations.

All proton-imaging studies were performed on a prototype General Electric MR system using a superconducting magnet operating at 1.5 T (15 kG). At least two standard pulse sequences were routinely used: (1) a multislice spin-echo pulse sequence with a repetition time (TR) of 2000 msec and an echo delay (TE) of 100 msec (SE 2000/100) to obtain T2-weighted information, and (2) a multislice spin-echo partial-saturation pulse sequence with a TR of 400 msec and a TE of 20 msec (PS 400/20) to obtain T1-weighted information.

In addition, 13 patients (ages 16 years to 63 years) also had a comprehensive single-slice, multiple spin-echo analysis at one or more brain levels using a TR of 1500 or 2000 msec and a TE of 25, 50, 75, and 100 msec. These multiple spin-echo data were used to calculate images of T2 as well as pseudodensity by performing a linear regression on the logarithms

This article appears in the May/June 1986 issue of *AJNR* and the July 1986 issue of *AJR*.

Received October 25, 1985; accepted after revision January 3, 1986.

Presented in part at the annual meeting of the American Society of Neuroradiology, New Orleans, February 1985.

[1] Department of Radiology, Duke University Medical Center, Durham, NC 27710. Address reprint requests to B. P. Drayer, Department of Radiology, Box 3808, Duke University Medical Center, Durham, NC 27710.

[2] Department of Medicine (Neurology), Duke University Medical Center, Durham, NC 27710.

[3] Department of Pathology, Duke University Medical Center, Durham, NC 27710.

***AJNR* 7:373–380, May/June 1986**
0195–6108/86/0703-0373

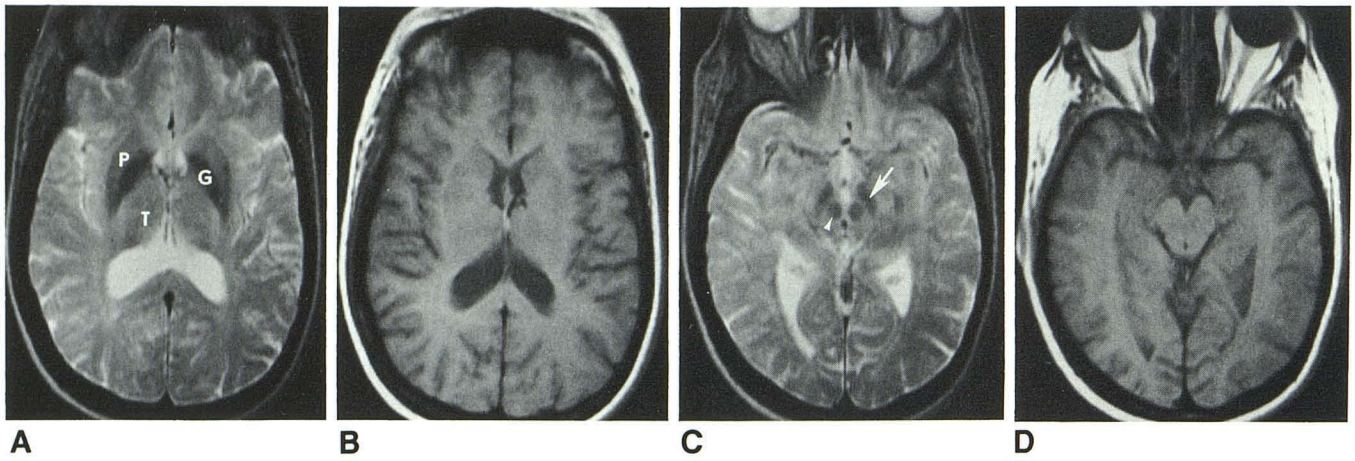

Fig. 1.—Normal brain iron, axial 1.5 T MR. **A**, SE 2000/100: decreased signal intensity (decreased T2, increased iron) prominently noted in the globus pallidum (G) as compared with the putamen (P) and thalamus (T) in this normal 43-year-old woman. **B**, PS 400/20: normal appearance at same basal ganglia level with expected decreased signal intensity (increased T1) in gray matter structures. **C**, SE 2000/100: decreased signal intensity (decreased T2, increased iron) in red nucleus (*arrowhead*) and reticular substantia nigra (*arrow*) in same patient. **D**, PS 400/20: the red nucleus and substantia nigra are not delineated on this T1-weighted image.

of the source signal values for each pixel. The negative reciprocal of the slope of the fitted line represents T2, while the exponential of the intercept represents pseudodensity [2]. Pseudodensity is equivalent to the signal that would be measured at a TE of zero. The fitting details are described more fully by MacFall [2]. The T2 values from normal regions of cortical gray and white matter, basal ganglia nuclei, internal capsule, thalamus, and lateral ventricles were then tabulated using the average value from operator-selected, specified regions of interest from the T2 maps. The regions of interest included 25 pixels in order to determine an accurate mean and standard deviation yet avoid excessive partial volume averaging. Owing to size constraints, the region of interest was limited to 9 pixels in the caudate, putamen, globus pallidum, and internal capsule.

A slice thickness of 5 or 10 mm was routinely used with a 128 (phase) × 256 (frequency) matrix size for both the single-slice and multislice acquisitions. All images were obtained using a single signal average (one average = two excitations). It therefore required 8 min and 32 sec to acquire a single-slice or multislice group of images with a TR of 2000 msec.

In addition to the MR studies, additional iron-staining experiments were performed on 12 other individuals. Formalin-fixed brains from normal individuals were washed in tap water for 15 min, rinsed with distilled water three times, and then immersed in Perl's solution for 30 min to determine the topographic distribution of ferric (Fe III) iron in the brain. At the end of 30 min, the staining solution was decanted and the specimens washed in running tap water for 5 min followed by black and white color photography. The Perls histochemical reaction results in a concentration-related blue intensity in areas of brain containing ferritin and other ferric compounds to which iron is loosely bound [3, 4]. The topographic distribution of iron was then studied in these postmortem brains from 12 neurologically intact individuals of the following ages: newborn (2), 1 year, 18 years, 21 years, 43 years, 44 years, 67 years, 70 years, 74 years, 76 years, and 84 years.

Results

Image Analysis

Discrete regions of decreased MR signal intensity on *SE 2000/100* images (decreased T2) were well visualized in the globus pallidum, red nucleus, pars reticulata of the substantia nigra, dentate nucleus of the cerebellum, and to a lesser degree in the putamen of every individual studied (Figs. 1 and 2). In addition, the signal intensity of the frontal white matter was consistently lower than that of the occipital visual white matter pathways. A focal area of mildly increased signal intensity was normally seen at the posterior border of the posterior limb of the internal capsule (retrolenticular). A subcortical white-matter ribbon of decreased signal intensity on the SE 2000/100 images was consistently seen most prominently in the temporal lobe on coronal images (Fig. 2).

The globus pallidum had a slightly higher signal intensity than the caudate or putamen on the *PS 400/20* msec images. The T1 of gray matter is normally higher than that of white matter (decreased signal intensity on PS 400/20 image). An increase in signal intensity was not seen in the red nucleus, substantia nigra, or dentate nucleus on the PS 400/20 images. In three individuals in whom *SE 6000/20 images* were obtained, the signal intensity in the globus pallidum was always lower than that in the caudate and putamen (Fig. 3), denoting a decreased spin density in the pallidum. A decreased signal intensity in the globus pallidum, substantia nigra, red nucleus, and dentate nucleus was also routinely noted on *SE 2000/30 images*, though not as prominently as on the SE 2000/100 series.

T2 Relaxation Time Estimations

The mean T2 relaxation times in 13 subjects estimated from 10-mm axial sections passing through the basal ganglia are summarized in Table 1. The lowest T2 value was found in the globus pallidum; intermediate T2 values were found in the putamen; and the highest T2 values were in the thalamus, caudate, cerebral gray, and cerebral white matter. The T2 of the occipital white matter was either equal to (4) or greater than (7) the frontal white matter in 11 of the 13 studies.

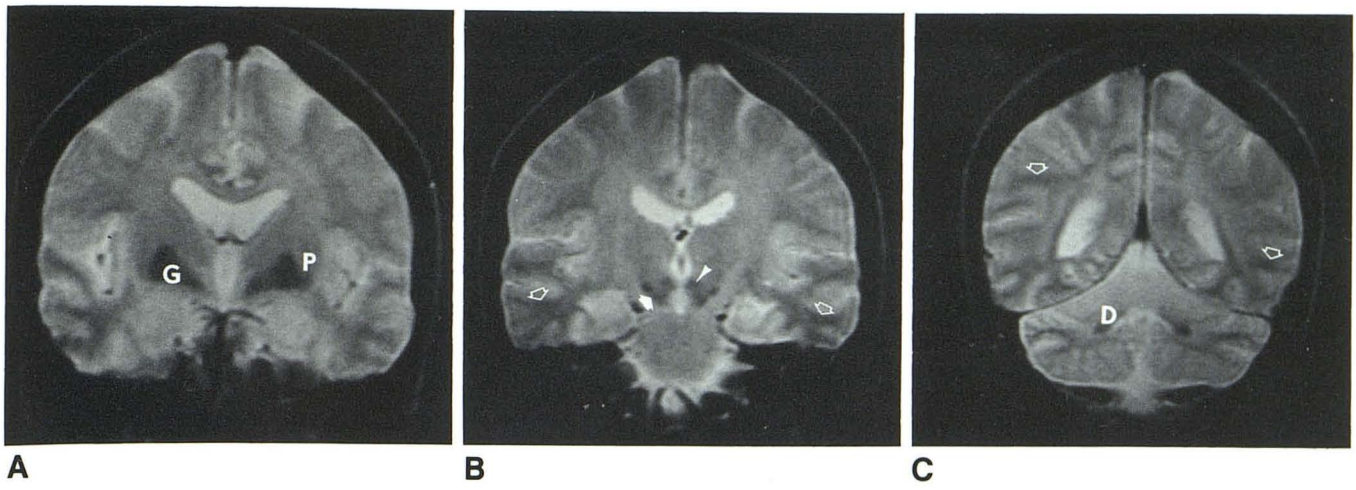

Fig. 2.—Normal brain iron, coronal 1.5 T MR. **A–C**, SE 2000/100 images in normal 48-year-old man clearly delineate regions of decreased signal intensity (decreased T2, increased iron) in the globus pallidum (G), putamen (P), red nucleus (*arrowhead*), reticular substantia nigra (*arrow*), dentate nucleus (D), and subcortical "U" fibers (*open arrows*).

Fig. 3.—Normal spin density image. Spin-density (PS 6000/20) weighted image shows the highest signal intensity in the putamen as fewer white matter tracts course through the putamen as compared with other basal ganglia nuclei.

TABLE 1: **Estimated T2 Relaxation Time, 13 Patients**

	Mean T2 (msec)[1]	SD (msec)	Range (msec)	Ratio vs. White
Cerebral white[2]	72	3.7	57–80	—
Cerebral gray[3]	73	2.5	59–79	1.01
Globus pallidum	60	2.5	49–70	.83
Putamen	68	1.3	54–79	.94
Thalamus	73	2.2	55–94	1.01

[1] T2 estimated from TR 1500 msec; TE 25, 50, 75, and 100 msec single-slice multiple spin-echo pulse sequence.
[2] Mean of 6 × 6 pixel region of interest in frontal and occipital white matter of each patient.
[3] Mean of four regions of interest in cerebral gray matter of each patient.

Neuropathologic Localization of Ferric Iron (Perls Stain)

The ferric iron was apparent as blue staining in a specific topographic distribution in all brains except for the two newborns. The brain from the one-year-old subject showed faint blue staining of both segments of the globus pallidum, the substantia nigra, and the red nucleus, but no staining was seen in the dentate nucleus, striatum, or thalamus. In the remaining nine brains, there was intense blue staining (increased ferric iron) in the globus pallidum, red nucleus, pars reticulata of substantia nigra, subthalamic nucleus, and dentate nucleus of the cerebellum (Fig. 4). Moderate blue staining was noted in the putamen, caudate. Ammon's horn, and thalamus, while only slight staining was seen in the centrum semiovale. The optic radiations were consistently unstained, and a thin ribbon of moderately intense blue staining coincided with the subcortical "U" fibers. With increasing age (e.g., brains from the 74-year-old, 76-year-old, and 84-year-old subjects), the blue intensity in the putamen was nearly as intense as in the globus pallidum, and the staining in the dentate nucleus of cerebellum was less discrete and spread into surrounding tissues (Fig. 5). The regions of decreased T2 relaxation time and decreased signal intensity on SE 2000/100 images coincided precisely with the sites of the most intense blue staining using the Perls method.

Tissue blocks from the basal ganglia, midbrain, and dentate nucleus were taken from four cases after sections were stained for iron, dehydrated, and embedded in paraffin. These sections were then cut and histologic sections stained for iron by the Perls method. All sections disclosed positive microscopic iron staining within the same regions in which ferric iron was seen macroscopically (Perls stain). The microscopic deposition of iron was within astrocytes, while no iron was seen within neurons.

Discussion

A decreased signal intensity on SE 2000/100 (T2-weighted) images was noted in specific anatomic locales in 150 consecutive patients studied with high field strength (1.5 T) MR imaging. This finding, as well as decreased calculated T2 measurements from 13 patients, correlated precisely with the highest concentration of ferric iron as determined by the Perls staining method on 12 normal postmortem brains. An under-

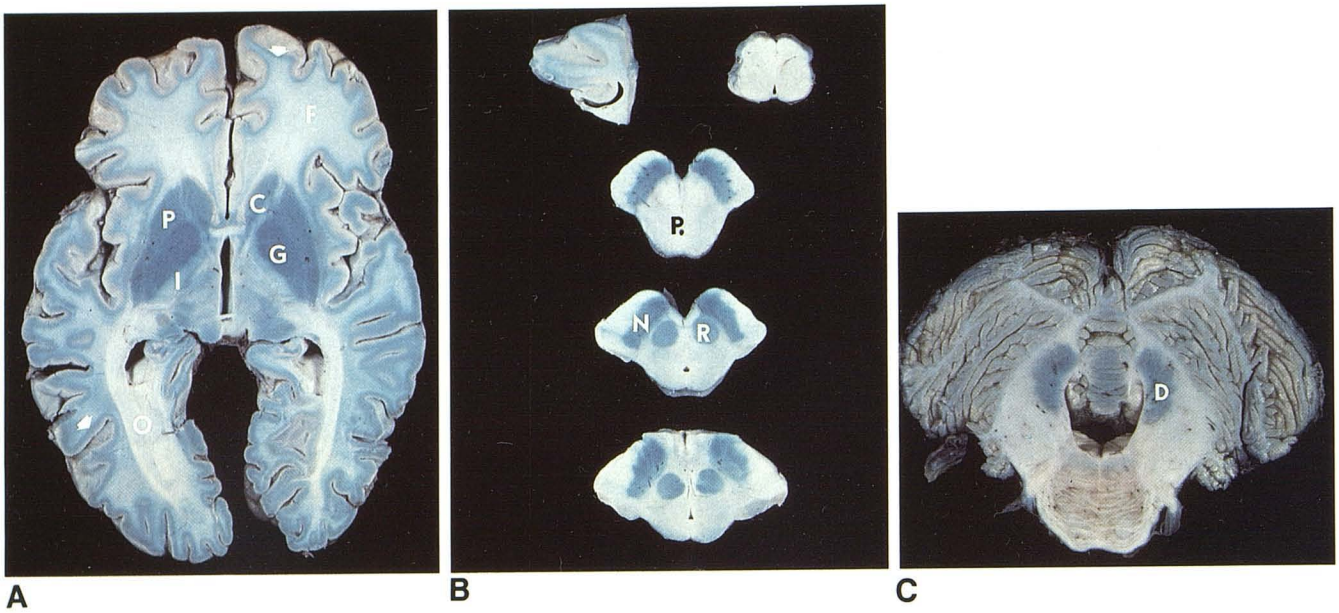

Fig. 4.—Perls stain of normal brain (44-year-old man). The greater intensity of blueness on the Perls stain represents the highest concentration of ferric iron correlating closely with regions of decreased signal intensity on high field MR. **A**, Globus pallidum (G), putamen (P), caudate (C), internal capsule (I), frontal white matter (F), optic radiations, (O), and subcortical "U" fibers (*arrow*). **B**, Red nucleus (R), substantia nigra (N), and periaqueductal gray matter (P). **C**, Dentate nucleus of the cerebellum (D).

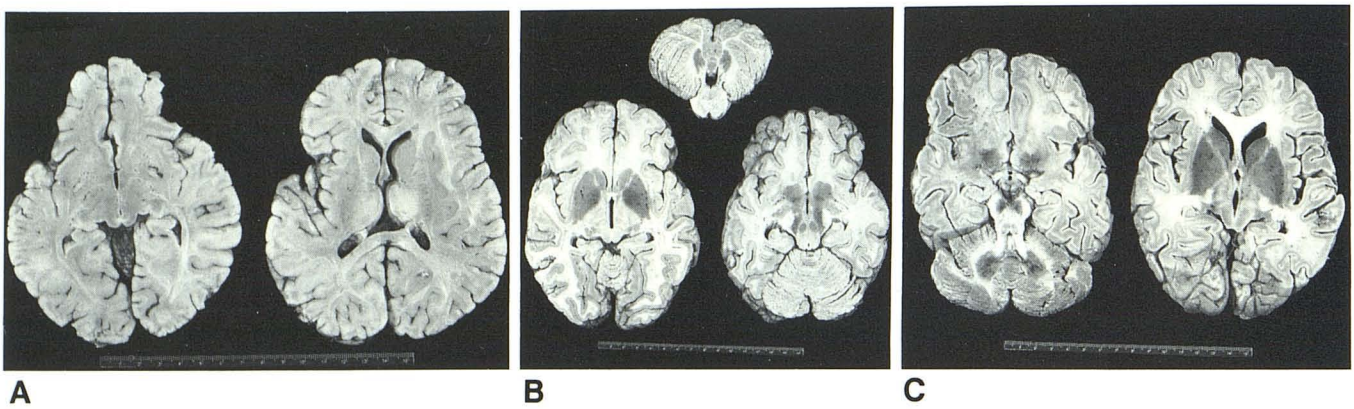

Fig. 5.—Perls stain of brain with normal aging. The greater intensity of grayness represents the highest concentration of ferric iron. **A**, One-year old: negligible brain iron. **B**, 43-year-old: normal distribution of ferric iron with highest concentrations in the globus pallidum, red nucleus, substantia nigra, and dentate nucleus and lower concentrations in the putamen, caudate, and subcortical "U" fibers. **C**, 84-year-old: the ferric iron concentration in the putamen and caudate equals that in the globus pallidum, and the iron in the dentate nucleus is no longer discrete.

standing of the normal distribution of brain iron may thus prove critical for the interpretation of high field strength MR images.

Brain Iron Distribution

Certain sites in the brain have a preferential accumulation of nonhaemin iron. Hallgren and Sourander [5] studied the distribution of iron in 81 normal brains at autopsy. They described a progressive increase in iron distribution that plateaus in the late teens or twenties with a second, milder increase after age 60. The normal sites of iron predilection from various pathologic studies [5–8] as well as our own are in decreasing order of frequency: the globus pallidum (20–25 mg Fe/100g), red nucleus, zona reticulata of the substantia nigra, subthalamic nucleus of Luys, dentate nucleus of cerebellum, and putamen. The caudate and thalamus contain lower concentrations of nonhaemin iron. The lowest iron concentrations are found in the cerebral and cerebellar hemispheric white and gray matter. The subcortical "U" fibers have a greater iron content than either the cerebral gray or white matter [5]. The frontal white matter has a greater iron distribution than the occipital white matter with almost no ferric iron in the most posterior portion of the posterior limb of the internal capsules and optic radiations.

Our study confirms that there is no detectable ferric iron in

the brain at birth, with iron stains first becoming positive at approximately 6 months of age in the globus pallidum. This is followed by staining in the reticular substantia nigra at 9 to 12 months, the red nucleus at 18 to 24 months, and the dentate nucleus at 3 to 7 years [6–8]. There is a mixture of granular and diffuse iron in the brain, and the granular iron increases progressively with age. Brain iron is likely independent of hemoglobin metabolism and the iron reserves of the remainder of the body. For example, the siderosis with hemochromatosis only occurs in areas of the brain that do not have a blood–brain barrier (e.g., neurohypophysis, pineal, area postrema, choroid plexus, infundibulum, subfornical body) [6].

Iron Metabolic Pathway

Iron is absorbed via the small bowel and is immediately bound to transferrin on entering the bloodstream. Transferrin transports iron to body cells but is not assimilated by the cell. When iron is incorporated into protoporphyrin IX, it is converted to heme iron and becomes a component of proteins, such as hemoglobin, myoglobin, cytochromes, catalase, and peroxidase. Nonhaemin iron attaches to hemosiderin, apoferritin, and ferritin, and in these forms is considered storage iron. Ferritin is derived from apoferritin when micellar iron enters the core of the molecule. Apoferritin is synthesized intracellularly by free and bound ribosomes, and its formation may be stimulated by the presence of iron. The amount of ferritin produced is dependent on the amount of iron available. Ferritin has a molecular weight of 480,000 with a crystalline ferricoxyhydroxide core containing 4000 ferric iron molecules in a high-spin state ($S = 5/2$), a protein shell, and recognition at electron microscopy as quadruplicate granules with a dense central core [6]. Ferritin does not cross the blood–brain barrier.

Monclonal antibodies against rat and human transferrin receptors label the luminal surface of brain capillary endothelial cells but not capillaries in the remainder of the body [9]. These receptors may allow the transport of transferrin, and thus iron, into the brain from the circulating blood. It is of interest that the greatest transferrin receptor density is not in regions of brain with the highest iron concentration but rather in areas that have their dominant projections to iron-rich locales [10]. This suggests that an axonal transport of iron may be made to regions of the brain requiring iron for specific metabolic activities. Hill et al. [10] have proposed that transferrin receptors are in the neuropil in molecular layers of laminated brain regions, at which sites iron transferrin is internalized by neuronal dendrites, transported along axons, and subsequently released and stored in oligodendrocytes.

Histochemical examinations by Diezel [7] revealed that a large part of the finely granular brain iron is present as *ferritin*, the most readily mobilizable form of storage iron. Hallgren and Sourander [5] found that the mitochondria and microsomes contain approximately half of the nonhaemin iron in the brain. Microscopically, fine granular deposits of iron are seen predominantly in glial cells and oligodendrocytes [4, 5], but they may also be seen in neurons, the neuropil, and inner and outer loops of myelin sheaths. The high iron content, solubility characteristics, typical electron microscopic appearance, electrophoretic mobility, stability to heat, and prominent staining with Perls histochemical reaction for ferric iron make it highly likely that the soluble iron-containing protein in the brain is predominantly ferritin [4–7, 11–13].

In addition to ferritin, brain iron is present in other forms. *Iron enzymes* play an important role in oxidative reactions [4, 6, 13–17]. For example, the enzyme DPNH-cytochrome-C-reductase has a high iron content. Iron and lactoflavin content of the brain are generally parallel except for low lactoflavin in the globus pallidum [6]. This suggests that iron-containing flavoproteins (DPNH dehydrogenase, succinic acid dehydrogenase) may play an important role in cellular respiration. The increased concentration of nonheme iron in the brain mitochondria and microsomes with aging suggests that this may reflect an alteration in enzyme systems of the cell (e.g., electron transport system of the mitochondria) [5, 18]. Biopsies of the VL nucleus of the thalamus from Parkinsonian patients have demonstrated iron impregnation of mitochondria that have been theorized to interfere with the electron transfer system and thereby the BBB leading to progressive accumulation of iron [19].

Brain Iron and Neurotransmitters

Iron may also play an important role in *neurotransmitter metabolism* [14–16]. Iron is a required cofactor for the monoamine synthetic and degradative enzymes tyrosine hydroxylase, tryptophan hydroxylase, and aldehyde oxidase; and it plays an important role in the maintenance of monoamine oxidase levels [17]. Iron is also involved in serotonin and dopamine receptor function [17]. Some of the neurologic symptomatology (e.g., poor attentiveness and control) associated with chronic iron deficiency anemia, especially in children, has been attributed to abnormal functioning of the dopamine system [14, 17, 20–22].

Hill and Switzer [4], using a Perls histochemical reaction for ferric iron intensified with diaminobenzidine, found a similar normal preferential distribution of brain iron in the globus pallidum, reticular zone of substantia nigra, interpeduncular nucleus, and dentate nucleus in rats. Of interest is that areas of highest monoamine concentration (e.g., caudate, zona compacta of substantia nigra) have only low to moderate iron concentrations. The globus pallidum and reticular substantia nigra (high iron locations) are efferent motor nuclei with high concentrations of gamma-aminobutyric acid (GABA) [23]. These similarities of iron and GABA distribution suggest that iron may play a role in GABA metabolism [4]. Hill [24] has recently reported a significant reduction in iron concentration in the homolateral ventral pallidum, globus pallidum, and substantia nigra 2 days after injecting gamma-vinyl GABA (enzyme-activated inhibitor of GABA transaminase) into the striatum/globus pallidum region. Glutamine binding is a precursor for GABA metabolism [25]. Iron is also a requirement for succinic dehydrogenase, the enzyme through which the product of the GABA shunt re-enters the citric acid cycle [26].

Metalloenzymes are also involved in the metabolism of

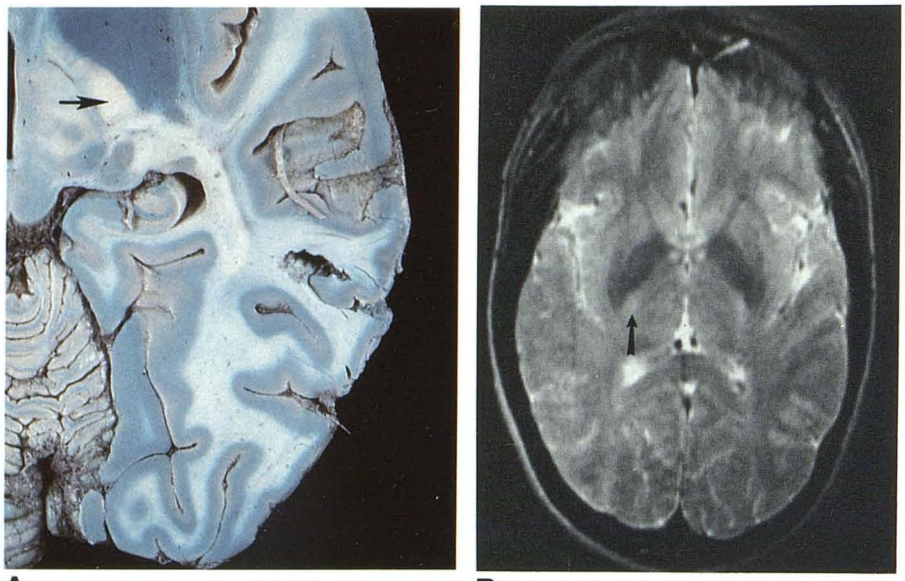

Fig. 6.—Perls stain and MR of normal brain. **A**, Perls stain shows absence of blue staining (i.e., ferric iron) in the posterior section of the posterior limb of the internal capsule (*arrow*). **B**, SE 2000/100 image from normal patient showing a normal increased signal intensity in the posterior portion of the posterior limb of the internal capsule due to absence of ferritin.

neuroactive peptides [27]. Enkephalin is abundant in high-iron-concentration sites (ventral pallidum, globus pallidum, interpeduncular nucleus) in the rat. However, many sites of lower iron concentration also have abundant enkephalin [28]. These anatomic similarities between GABA, enkephalin, and iron distribution in specific brain locales suggest that iron may be associated with neurotransmitter or neuroactive peptide metabolism, and that the gradual increase of iron with age may relate to storage of metabolic products with iron.

Iron and Aging Brain

Iron may play an important role in the *normal aging* process. Dismutation of O_2 leads to production of hydrogen peroxide (H_2O_2), which readily crosses cell membranes [29]. When H_2O_2 comes in contact with ferrous (II) iron, highly reactive hydroxyl radicals and ferric (III) iron are produced. Low-molecular-weight iron complexes (e.g., iron-citrate, iron-ATP), rather than storage iron (ferritin), are the major catalysts of this reaction [29]. Hydroxyl radicals initiate lipid peroxidation, which causes a loss of membrane permeability to calcium with its associated cellular toxicity. This series of reactions may be prevented by removing metal ions, e.g., iron chelation with desferrioxamine, which binds ferric salts in a form that cannot be reduced by superoxides [30].

Iron and Brain Disorders

There is strong neuropathologic evidence that various degenerative disorders involving the central nervous system are associated with an increase in brain-iron deposition. The disorder in which increased iron is most firmly established is neuroaxonal dystrophy or *Hallervorden-Spatz* disease [6]. There is extensive iron deposition in the globus pallidum and reticular zone of the substantia nigra that is far in excess of that seen in these normally high-iron locations. In addition, iron may catalyze pseudoperoxidation of lipofuscin into neuromelanin, which is largely responsible for the pigmentary accumulations in Hallervorden-Spatz [31, 32].

Many other disorders of the central nervous system have been associated with an excessive deposition of iron in specific brain locales. Excessive iron deposition has been reported in *Huntington's disease* [33] (caudate, putamen), *Parkinson's disease and multisystem atrophy variants* [19, 34–36] (putamen, globus pallidum), *Alzheimer's disease* [18] (cerebral cortex), *multiple sclerosis* [37] (adjacent to plaques), *radiation effects* [6] (vascular endothelium), *chronic hemorrhagic cerebral infarction* [6] (ferrugination), and *intracerebral hematoma periphery* [6] (macrophage-laden ferritin and hemosiderin accumulation occurs within 24 hr). The ability to precisely map the distribution of iron in the brain in vivo may therefore provide important new insights into the diagnosis and pathophysiology of the brain damage that occurs in association with neurodegenerative, demyelinating, and vascular disorders.

An understanding of the normal brain-iron distribution may also help interpret high field strength T2-weighted MR images—even in diseases that are not associated with abnormal iron deposition—by highlighting normal anatomic landmarks. The absence of iron in the most posterior portion of the posterior limb of the internal capsule and optic radiations explains the relatively increased signal intensity often seen in this location on long TR and TE (e.g., SE 2000/100 msec) pulse sequences (Fig. 6). The frontal white matter has a lower signal intensity than the occipital white matter because of higher iron concentration. On coronal SE 2000/100 images, the temporal-lobe white matter has a lower signal intensity than the frontal or parietal white matter because of partial volume effects from the closer proximity of iron-containing

subcortical "U" fibers in the temporal lobe. The characterization of vasogenic edema or demyelinating disorders as involving only white matter is simplified owing to sparing of the decreased-signal-intensity, iron-containing, basal ganglia nuclei.

Iron and T2 Relaxivity

The question arises as to whether the prominent decrease in T2 in the described locations on high field strength imaging is definitely related to iron accumulation. Calcium may increase with age in the globus pallidum and dentate nucleus, but it does not accumulate in significant quantities in the red nucleus or substantia nigra. The structures that have decreased signal intensity on the T2-weighted images have an intensity comparable to cerebral gray matter on non-T2-weighted images. Melanin has only a mild effect on T1 relaxivity and a different topographic distribution. Lipofuscin has a similar anatomic localization, but will not significantly and specifically affect T2 relaxivity. Iron is the only trace metal in the brain that can prominently and preferentially decrease the T2 relaxation time and localize in precisely the topographic basal ganglia regions seen on the high field strength MR images.

The marked dominance of the T2 effect is fully in keeping with the presence of ferric iron in the brain. Stark et al. [38] reported a similar T2 relaxivity dominance with hepatic iron overload. The decreased T2 in the absence of decreased T1 is a consequence of increased localized ferritin in the described basal ganglia regions. The crystalline ferricoxyhydroxide core of ferritin has up to 4000 ferric ions per molecule and is encased by an approximately 25-angstrom protein shell. Theories of outersphere relaxation would suggest no significant alteration in the T1 or T2 relaxation time using proton MR. However, intracellular iron causes slow statistical fluctuations in the magnetization of each ferritin core giving rise to local magnetic field gradients and inhomogeneities [39–42]. Water molecules diffusing in the region of the ferritin molecule will experience a relatively static magnetic field resulting in line broadening on the proton chemical shift spectra, a significant decrease in the transverse relaxation (T2) without affecting the longitudinal relaxation (T1), and a resulting decrease in signal intensity on an SE 2000/100 msec (T2-weighted) image. In essence, the protons in an area of the brain with a high ferritin content (e.g., globus pallidum) encounter a local, static magnetic field (heterogeneity in magnetic susceptibility) that is larger than anticipated, and the resulting T2 is therefore less. This statistical fluctuation is proportional to the square of the magnetic field strength, which explains the difficulty in visualizing normal concentrations of brain iron at lower field strengths.

By monitoring the decreased signal intensity on T2-weighted images in specific brain locales (e.g., globus pallidum, red nucleus, reticular substantia nigra, dentate nucleus) and by understanding the large, slow statistical variations in the magnetization of the ferritin core resulting in a large, relatively static local magnetic field, routine MR imaging can be used to create a map of brain ferric iron distribution in a living subject. This new, in vivo, biochemical application of proton MR should facilitate new, dynamic insights into the normal selectivity of iron for preferential sites in the brain and also provide a new tool to assist in the diagnosis and understanding of many disorders involving the central nervous system [43].

REFERENCES

1. Drayer BP, Burger P, Riederer S, et al. High resolution magnetic resonance imaging for mapping brain iron deposition (abstr). *AJNR* **1985**;6:466
2. MacFall JR. Pulse sequence considerations for computed T1, T2, and spin density images. In: Essen PD, Johnston RE eds. *Technology of nuclear magnetic resonance.* New York: Society of Nuclear Medicine, **1984**:79.
3. Perls M. Nachweis von Eisenoxyed in giwissen Pigmenten. *Virchow Arch [A]* **1867**;39:42–48
4. Hill JM, Switzer RC III. The regional distribution and cellular localization of iron in the rat brain. *Neuroscience* **1984**;11:595–603
5. Hallgren B, Sourander P. The effect of age on the non-haemin iron in the human brain. *J Neurochem* **1958**;3:41–51
6. Seitelberger F. Pigmentary disorders. In: Minckler J ed. *Pathology of the nervous system.* New York: Blakiston Division, McGraw Hill, **1972**:1324–1338
7. Diezel PB. Iron in the brain: a chemical and histochemical examination. In: *Biochemistry of the developing nervous system.* New York: Academic Press, **1955**:145–152
8. Cumings JN. The copper iron content of brain and liver in the normal and hepatolenticular degeneration. *Brain* **1948**;71:410–415
9. Jefferies WA, Brandon MR, Hunt SV, William AF, Gatter KC, Mason DY. Transferrin receptor on endothelium of brain capillaries. *Nature* **1984**;312:162–163
10. Hill JM, Ruff MR, Weber RJ, Pert CB. Transferrin receptors in rat brain: neuropeptide-like pattern and relationship to iron distribution. *Proc Natl Acad Sci USA* **1985**;82:4553–4557
11. Francois C, Nguyen-Legros J, Percheron G. Topographical and cytological localization of iron in the rat brain. *Neuroscience* **1984**;11:595–603
12. Mulligan M, Linder M. The size of small molecular weight iron polls in rat tissue. In: Saltman P, Hagenaeuer J eds. *The biochemistry of physiology of iron.* New York: Elsevier Biomedical, **1982**:313–314
13. Rafaelsen OJ, Rofod B. Iron. In: Lajtha A ed. *Handbook of neurochemistry*, Vol 6. Plenum Press, **1969**:261–271
14. Mackler B, Parson R, Miller LR, Inamdar AR, Finch OA. Iron deficiency in the rat. Biochemical studies of brain metabolism. *Pediatr Res* **1978**;12:217–224
15. Sourkes TL. Transition elements and the nervous system. In: Pollitt E, Leibel RL eds. *Iron deficiency: brain biochemistry and behavior.* New York: Raven Press, **1982**:1–29
16. Youdim MBH, Green AR, Bloomfield MR, Mitchell BD, Heal DJ, Grahame-Smith DG. The effects of iron deficiency on brain biogenic monoamine bochemistry function in rats. *Neuropharmacology* **1980**;19:259–267
17. Youdim MBH, Yehuda S, Ben-Shachar D, Ashkenazi R. Behavioral and brain biochemical changes in iron deficient rats: the involvement of iron and dopamine receptor function. In: Pollitt E, Leibel RL eds. *Iron deficiency: brain biochemistry and behavior.* New York: Raven Press, **1982**:39–56
18. Hallgren B, Sourander P. The non-haemin iron in the cerebral

cortex in Alzheimer's disease. *J Neurochem* **1960**;5:307–310
19. Rojas G, Asenjo A, Chiorino R, Aranda L, Rocamora R, Donoso P. Cellular and subcellular structure of the ventrolateral nucleus of the thalamus in Parkinson disease. Deposits of iron. *Confin Neurol* **1965**;26:362–376
20. Dallman PR, Siimes MA, Maines EC. Brain iron: persistent deficiency following short-term iron deprivation in the young rat. *Br J Haematol* **1975**;31:209–215
21. Leibel R, Greenfield D, Pollitt E. Biochemical and behavioral aspects of sideropenia. *Br J Haematol* **1979**;41:145–150
22. Youdim MBH, Yehuda S, Ben-Uria Y. Reversed circadian rhythm of dopaminergic mediated behaviors and thermoregulation in rats produced by iron deficiency. *Eur J Pharmacol* **1981**;4:295–301
23. Fahn S. Regional distribution studies of GABA and other putative neurotransmitters and their enzymes. In: Roberts E, Chase TN, Tower DB eds. *GABA and nervous system function.* New York: Raven Press, **1976**:169–186
24. Hill JM. Pallidal and nigral iron concentration reduced by gamma-vinyl GABA (abstr). *Soc for Neurosci* **1984**;10:974
25. Michaelis EK, Belieu RM, Grubbs RD, Michaelis ML, Chang HH. Differential effects of metal ligands on synaptic membrane glutamate binding uptake systems. *Neurochem Res* **1982**;7:423–436
26. Frieden E. The evaluation of metals as essential elements. In: Friedman M ed. *Protein-metal interactions.* New York: Plenum Press, **1974**:1–32
27. Sullivan S, Akil J, Blacker D, Barchas JD. Enkephalinase: selective inhibitors and partial characterization. *Peptides* (Fayetteville) **1980**;1:31–35
28. Sar M, Stumpf WE, Miller RJ, Chang K, Cuatrecasas P. Immunohistochemical localization of enkephalin in rat brain and spinal cord. *J Comp Neurol* **1978**;182:17–38
29. Halliwell B, Gutteridge JMC. Oxygen radicals and the nervous system. *TINS* **1985**;22–26
30. Gutteridge JMC, Richmond R, Halliwell B. Inhibition of the iron-catalysed formation of hydroxyl radicals and of lipid peroxidation by desferrioxamine. *Biochem J* **1979**;184:469–472
31. Park BE, Netsky MG, Betsill WL. Pathogenesis of pigment and spheriod formation in Hallervorden-Spatz syndrome and related disorders. *Neurology* **1975**;25:1172–1178
32. Jankovic J, Kirkpatrick JB, Blomquist KA, Langlaid PJ, Bird ED. Late-onset Hallervorden-Spatz disease presenting as familial parkinsonism. *Neurology* **1985**;35:227–234
33. Klintworth GK. Huntington's chorea—morphologic contributions of a century. In: *Advances in neurology.* New York: Raven Press, **1973**:353–368
34. Earle KM. Studies on Parkinson's disease including x-ray, fluorescent spectroscopy of formalin-fixed brain tissue. *J Neuropathol Exp Neurol* **1968**;27:1–14
35. Lhermitte J, Kraus WM, McAlpine D. Etude des produits de desintegration et des depots du globus pallidus dans un cas de syndrome parkinsonien. *Rev Neurol* (Paris) **1924**;1:356–361
36. Borit A, Rubinstein J, Urich H. The striatonigral degenerations. *Brain* **1975**;98:101–112
37. Craelius W, Migdal MW, Luessenhop CP, Sugar A, Mihalakis I. Iron deposits surrounding multiple sclerosis plaques. *Arch Pathol Lab Med* **1982**;106:397–399.
38. Stark DD, Moseley ME, Bacon BR, et al. Magnetic resonance imaging and spectroscopy of hepatic iron overload. *Radiology* **1985**;154:137–142
39. Robertson B. Spin-echo decay of spines diffusing in a bounded region. *Physiol Rev* **1966**;151:273–277
40. Packet KJ. The effects of diffusion through locally inhomogeneous magnetic fields on transverse nuclear spin relaxation in heterogeneous systems: proton transverse relaxation in striated muscle tissue. *J Magn Reson* **1973**;9:438–443
41. Brittenham GM, Farrell DE, Harris JW. Magnetic susceptibility measurements of human iron stores. *N Engl J Med* **1982**; 307:1671–1675
42. Koenig SH. A theory of solvent relaxation by solute clusters of noninteracting paramagnetic ions, as exemplified by ferritin (abstr). Society of Magnetic Resonance in Medicine **1985**;2:873–874
43. Drayer BP. Neurometabolic applications of magnetic resonance. ACR Categorical Course on Magnetic Resonance (Syllabus) **1985**;185–211